JCIM JOURNAL OF CHEMICAL INFORMATION AND MODELING

Letter

The Irony of Manganocene – An Interplay Between the Jahn-Teller Effect and Close Lying Electronic and Spin States

Stepan Stepanovic, Matija Zlatar, Marcel Swart, and Maja Gruden

J. Chem. Inf. Model., **Just Accepted Manuscript** • DOI: 10.1021/acs.jcim.8b00870 • Publication Date (Web): 18 Jan 2019

ACS Publications

is published by the American Chemical Society. 1155 Sixteenth Street N.W., Washington, DC 20036

The Irony of Manganocene – An Interplay Between the Jahn-Teller Effect and Close Lying Electronic and Spin States

Stepan Stepanović[1], Matija Zlatar[1], Marcel Swart[2,3], Maja Gruden[4*]

[1]Department of Chemistry, Institute of Chemistry, Technology and Metallurgy, University of Belgrade, Studentski trg 12-16, Belgrade, Serbia

[2]Institut de Química Computacional i Catàlisi (IQCC) and Departament de Química, Universitat de Girona, Campus Montilivi, Facultat de Ciències, 17003 Girona, Spain

[3]ICREA, Pg. Lluís Companys 23, 08010 Barcelona, Spain

[4] University of Belgrade - Faculty of Chemistry, Studentski trg 12-16, Belgrade, Serbia

Supporting Information Placeholder

ABSTRACT: Although the unusual structural, magnetic, electronic and spin characteristics of manganocene has intrigued scientists for decades, a unified explanation and rationalization of its properties has not yet been provided. Results obtained by Multideterminantal Density Functional Theory (MD-DFT), Energy Decomposition Analysis (EDA) and Intrinsic Distortion Path (IDP) methodologies, indicate how this uniqueness can be traced back to the manganocene's peculiar electronic structure, mainly, the degenerate ground state and close lying electronic and spin states.

Manganocene ($MnCp_2$) is an organometallic compound that has many unusual properties and manifests several characteristics that are completely unique regarding all other known cyclopentadienyl (Cp) sandwich compounds. $MnCp_2$ and its derivatives are the only metallocenes with spin crossover properties and chemical reactivity that correspond to those observed with pure ionic alkaline-earth metallocenes.[1-3] Furthermore, the antiferromagnetic behavior manifested below 159˚C, in the crystalline state, was very confusing with no analogy with previously, or subsequently discovered sandwich compounds.[1,4,5] Only after the elucidation of the microscopic structure, consisting of the intriguing polymer like a zigzag chain, Figure 1, did the observed magnetic properties become clear.[4] In the brown crystalline form, that exists below 159˚C, every manganese ion is coordinated with one η^5 cyclopentadienyl anion and two additional bridging Cp^- ligands, that achieve contact between neighboring manganese centers, a necessary prerequisite for the antiferromagnetic interaction. Manganocene is a thermochromic compound, and, at 159˚C an abrupt phase transition occurs to a pink crystalline form which persists until the $MnCp_2$ melting point at 175˚C.[6] In this paramagnetic pink form, and in the liquid and gas phase, manganocene molecules are in the common sandwich-like arrangement, with the high spin (HS) manganese center (S=5/2). In the monomeric sandwich arrangement, the low spin (LS) state is very close in energy, and it was expected that manganocene possesses spin crossover properties that could be observed by preserving the monomeric form at lower temperatures. In order to avoid the formation of a polymeric chain, the frozen solution was prepared (by doping in a host matrix of $MgCp_2$ and $FeCp_2$ below -183˚C) and, as anticipated, the LS state was observed.[1,7] However, the LS-HS energy difference was so small that even slight variations of intermolecular interactions in the frozen solutions were sufficient to change the ground state (depending on whether the host systems favor packing with long or short Mn-Cp distances).[1] At low temperature in a non-coordinating solvent (toluene) the equilibrium between the spin states and polymerization process was described.[8] Additionally, a spin-crossover temperature (-61˚C) for the monomeric form has been determined. All these results unequivocally demonstrated that monomeric units are LS, but switch to HS when increasing the temperature, and, when there is sufficient concentration and mobility of $MnCp_2$ units, the polymerization occurs, Figure 2.

Surprisingly, the isoelectronic ferrocenyl cation, $[FeCp_2]^+$, that has the same ground state, is found only in the monomeric LS form and shows none of the strange manganocene behavior.[9]

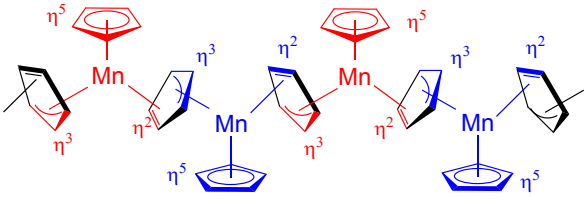

Figure 1. Schematic representation of the zigzag chain structure of $MnCp_2$. The different hapticity in shared rings is also depicted.

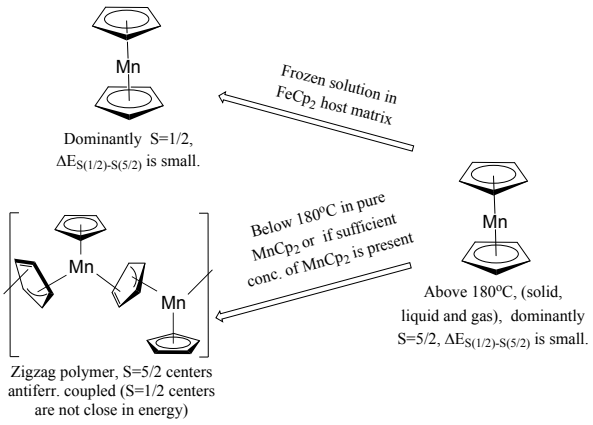

Figure 2. Schematic explanation of various forms of $MnCp_2$

Although the puzzling structural, magnetic, electronic and spin characteristics of manganocene intrigued scientists for many decades, an explanation for its unique properties, and reasons behind them, has not yet been provided. Instead, various interesting aspects of $MnCp_2$ behavior have been treated separately.[5,10-13] To the best of our knowledge, this is the first attempt to give an integrated approach accounting for all these phenomena and place them in the framework of the quantitative, but straightforward electronic structure arguments, by means of Density Functional Theory (DFT). It will be demonstrated that the peculiar behavior of $MnCp_2$ originates from its even more interesting electronic structure: mainly, the degenerate ground state and close lying electronic and spin states, by analysis of the spin states in the monomeric and zigzag environment, as well as the magnetic interactions between manganese centers when they are bridged with Cp^- ligands in the chain polymeric form. Through the entire manuscript, the correspondence has been made with the isoelectronic $[FeCp_2]^+$, which does not show the same behavior as manganocene.

The qualitative molecular orbital (MO) diagram of simple sandwich metallocenes, depicted in Figure 3, can be found in almost any inorganic/organometallic textbook.[6] In the D_{5h} symmetry the most important MOs, originating from five metal *d*-orbitals, are e_2', a_1' and e_1'' (Figure S1 in the Supplementary Information (SI)). e_2' and a_1' are metal centered, non-bonding and close in energy, while e_1'' are metal-ligand antibonding and much higher in energy, Figure S2. From this set of orbitals, in the case of a d^5 metal center, there are three important electronic configurations: $(e_2')^{\uparrow\downarrow\uparrow}(a_1')^{\uparrow\downarrow}(e_1'')$ i.e. $^2E_2'$ state, $(e_2')^{\uparrow\downarrow\uparrow\downarrow}(a_1')^{\uparrow}(e_1'')$ i.e. $^2A_1'$ state and $(e_2')^{\uparrow\uparrow}(a_1')^{\uparrow}(e_1'')^{\uparrow\uparrow}$ that gives $^6A_1'$ state. In the LS state, the $^2E_2'$ is the ground state, and is subject to Jahn-Teller (JT) distortion by e_1' vibrations, from D_{5h} to C_{2v}. If we consider an arrangement belonging to the D_{5d} symmetry, i.e. a staggered conformation of the Cp^- rings, the ground state is $^2E_{2g}$, inducing the distortion along the e_{1g} normal modes which removes the degeneracy and reduces the symmetry to C_{2h}. However, this conformation is less stable. The additional point that needs to be considered when analyzing the $MnCp_2$ electronic structure is the very close lying $^2A_1'$ state. It was initially even believed that $^2A_1'$ is the lowest doublet state in the gas phase.[1]

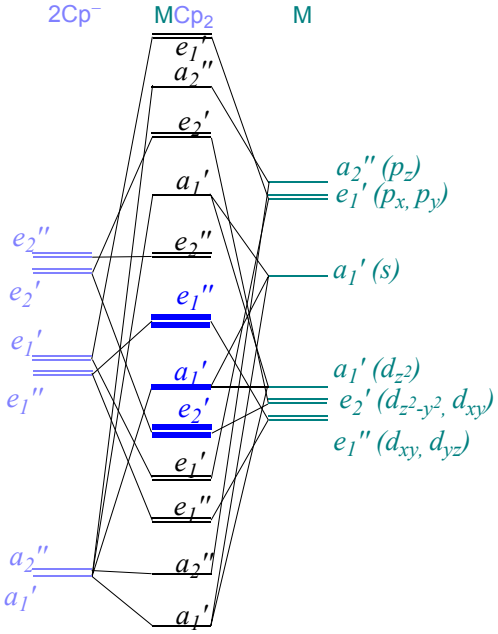

Figure 3. Qualitative MO diagram for metallocene sandwich compounds in D_{5h} symmetry.

All calculations have been done at OPBE/TZP level of theory, as implemented in ADF.[14] This level of theory afforded excellent results in the past, for both geometries and spin states of complicated transition metal compounds,[15-22] including metallocenes.[3] It is noteworthy that treatment of degenerate states by DFT is not straightforward, but multideterminantal DFT approach (MD-DFT) can be successfully applied.[23-25] Energies of degenerate states have been obtained using the high symmetry structure with the electronic density relaxed to a low symmetry subgroup[26] (see SI for details). The Mn-$Cp^{ring\ center}$ distances are 2.056Å for $^6A_1'$ state and 1.69Å for $^2E_2'$ state, and they are (as well as other structural parameters) in excellent agreement with the experimental values at elevated temperatures, Table S1.[27] The problem of accurate determination of the correct spin ground state by DFT in transition metal complexes was initially detected in 2001[28,29] and is perfectly demonstrated for the example of $MnCp_2$.[3,11,13,30] The abundance of theoretical work over the last two decades clearly indicated the preference of most hybrid functionals toward HS and early GGAs toward LS states.[16,22,28,31,32] Thus, since hybrids are often used and as $MnCp_2$ has a very close lying HS state, it is not a surprise that in several studies,[11,30] $MnCp_2$ is calculated to be in a HS ground state. With OPBE, proven to be accurate for spin state energetics, the LS state is preferential, with ΔE_{HS-LS}=5.00 kcal·mol^{-1}. This result is in perfect agreement with high-level *ab initio* calculations (ΔE_{HS-LS}(RASPT2)=4.93 kcal·mol^{-1}).[33] The energy difference between the $^2E_2'$ and $^2A_1'$ states was a more formidable task, and OPBE showed that $^2E_2'$ is lower in energy by just 0.05 kcal·mol^{-1}. In order to estimate the HS/LS energy difference in the zigzag polymeric chain, the $MnCp_3$ and a "trimer" with two Mg^{2+} ions around Mn^{2+} center, were used, Figure 4. The initial structures were taken from the $MnCp_2$ zigzag crystal structure, and then further relaxed. Using the geometry from the X-ray structure, as well as the optimized one, with both model systems, the very large HS/LS splitting in favor of the HS state was obtained (approximately -60 kcal·mol^{-1} in the X-ray environment and -35 kcal·mol^{-1} after relaxation).

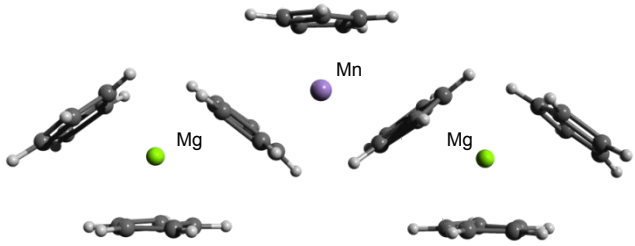

Figure 4. The model system used to estimate the HS/LS energy difference, on a single Mn^{2+} center in the zigzag structure.

As the ground state $^2E_2'$ is JT active, the JT stabilization energy (E_{JT}) was obtained by MD-DFT,[23-25] and the result of 1.43 kcal·mol^{-1} (500 cm^{-1}) corroborates the experimentally estimated value of 350 cm^{-1}.[34,35] The exchange coupling constant (see SI for details) calculated for a dimer extracted from the crystal structure was -15.5 cm^{-1}, which is in agreement with an experimental estimate of -9.3 cm^{-1},[4] representing the antiferromagnetic behavior. For the already described reasons, the comparison with $[FeCp_2]^+$ is given. The calculated values for the $^6A_1'/^2E_2'$ energy difference, $^2E_2'/^2A_1'$ energy difference and the E_{JT} for $[FeCp_2]^+$ are 46.95 kcal·mol^{-1}, -5.48 kcal·mol^{-1} and 1.32 kcal·mol^{-1} (462 cm^{-1}), respectively. These results indicate that $^2E_2'$ is more stabilized compared to both $^6A_1'$ and $^2A_1'$ states, but the E_{JT} is somewhat smaller than in the case of $MnCp_2$. However, these

results on their own were not enough to explain the differences between manganocene and the ferrocenyl cation.

In order to tackle the quantum mechanical reasons for the formation of zigzag polymer in $MnCp_2$, and not in $[FeCp_2]^+$, the thermodynamics of the zigzag environment has been examined. The first part of the analysis is devoted to the energy decomposition analysis.[36] In order to study the environment in the polymeric chain, the sandwich $MnCp_2$ is compared to the $MnCp_3$ model system (and analogously for Fe^{3+} in the ferrocenyl cation). The interaction of selected fragments (in our analysis, metal ion and Cp ligands) can be decomposed into two contributions: $\Delta E=\Delta E_{prep}+\Delta E_{int}$, The preparation energy, ΔE_{prep}, is the energy needed to prepare the ionic fragments and consists of three terms $\Delta E_{prep}=\Delta E_{deform}+\Delta E_{cyc\text{-}cyc}+\Delta E_{valexc}$. ΔE_{deform} is the energy needed to deform the separate Cp rings from their minimum energy structure to the geometry that they obtain in MCp_2, $\Delta E_{cyc\text{-}cyc}$ is the electrostatic repulsion between the two anionic Cp rings created while constructing one fragment with 2Cp rings. ΔE_{valexc} is the valence-excitation energy, needed to prepare the metal from its spin-unrestricted (polarized) ionic state (^6S for Mn^{2+} and Fe^{3+}) to the spin-restricted form used as a fragment file. The second contribution of the total energy is the interaction energy, ΔE_{int} , which is the energy released when the prepared fragments (i.e. Mn^{2+}(or Fe^{3+}) + 2Cp) are placed into the position they possess in MCp_2, and it also consists of three terms: $\Delta E_{int}=\Delta V_{elstat}+\Delta E_{Pauli}+\Delta E_{orbint}$. The term ΔV_{elstat} corresponds to the classical electrostatic interaction between the charge distributions of initial fragments, and is normally stabilizing. ΔE_{Pauli} (the Pauli-repulsion) represents the destabilizing contribution originating from the unfavorable interaction between fully occupied orbitals (since they produce both bonding and antibonding orbital fully occupied, but antibonding brings more destabilization); the combination of $\Delta V_{elstat}+\Delta E_{Pauli}$ is sometimes taken as measure for steric interactions. The orbital interaction ΔE_{orbint} incorporates several contributions, including donor–acceptor interactions (occupied orbitals on one fragment and unoccupied on the other). ΔE_{orbint} can be decomposed into the contributions from each irreducible representation.

Our EDA analysis (Tables 1 and 2) indicates that when we decompose the HS/LS energy difference, we see that the largest contribution to the HS/LS preference in $MnCp_3^-$ (compared to $MnCp_2$) comes from $\Delta E_{cyc\text{-}cyc}$ (which is more than twice as large in $MnCp_3^-$), i.e. the energy required to bring two (or three) Cp^- anions next to each other to the geometry of the complex. Since the dominant factor that governs the HS/LS preference is now extracted, this contribution for Fe^{3+} has been calculated and compared with Mn^{2+} results, as an attempt to explain the preference only of Mn^{2+} toward zigzag crystal structure. The results are given in Table 3. It is clear that the repulsion between Cp^- anions is comparable in $[FeCp_2]^+$ and $MnCp_2$, while for model systems with $3Cp^-$ anions these values differ by ~20 kcal·mol^{-1}. i.e. as distinct from D_{5h} structures, it is thermodynamically much less favorable to produce the zigzag form with Fe^{3+} than with Mn^{2+}.

Table 1. EDA analysis of $[Mn(Cp)_3]^-$ at OPBE/TZ2P level of theory, in kcal·mol^{-1}.

$[Mn(Cp)_3]^-$	LS	HS	ΔE
ΔE_{prep}	415.83	218.41	-197.42
ΔE_{deform}	1.34	0.38	-0.96
ΔE_{valexc}	159.28	1.89	-157.39
$\Delta E_{cyc\text{-}cyc}$	255.21	216.14	-39.07
ΔE_{int}	-972.19	-808.08	164.11
ΔE_{Pauli}	276.50	99.60	-176.90
ΔE_{elstat}	-724.56	-650.71	73.85
Total steric	-448.06	-551.11	-103.05
ΔE_{orbint}	-524.12	-256.98	267.14
$\Delta E_{HS\text{-}LS} = (\Delta E_{prep}+\Delta E_{int})_{HS}-(\Delta E_{prep}+\Delta E_{int})_{LS}=$			-33.31

Table 2. EDA analysis of $Mn(Cp)_2$ at OPBE/TZ2P level of theory. LS has been calculated in C_{2v} symmetry, since it is JT active. All values are in kcal·mol^{-1}.

$Mn(Cp)_2$	LS	HS	ΔE
ΔE_{prep}	248.76	78.43	-170.33
ΔE_{deform}	0.52	0.22	-0.30
ΔE_{valexc}	153	1.89	-151.11
$\Delta E_{cyc\text{-}cyc}$	95.24	76.32	-18.92
ΔE_{int}	-827.29	-650.42	176.87
ΔE_{Pauli}	298.08	120.14	-177.94
ΔE_{elstat}	-606.45	-533.84	72.61
Total steric	-308.37	-413.7	-105.33
ΔE_{orbint}	-518.92	-236.72	282.2
$\Delta E_{HS\text{-}LS} = (\Delta E_{prep}+\Delta E_{int})_{HS}-(\Delta E_{prep}+\Delta E_{int})_{LS}=$			6.5

Table 3. Comparison of $\Delta E_{cyc\text{-}cyc}$ for $[MCpn]^q$, for M = Mn^{2+}, Fe^{3+}, n = 2,3 and q = -1,0,+1. The values are in kcal·mol^{-1}.

		LS	HS
$MnCp_2$	$\Delta E_{cyc\text{-}cyc}$	95.24	76.32
$[FeCp_2]^+$	$\Delta E_{cyc\text{-}cyc}$	95.96	81.19
$[MnCp_3]^-$	$\Delta E_{cyc\text{-}cyc}$	255.21	216.14
$[FeCp_3]$	$\Delta E_{cyc\text{-}cyc}$	267.29	240.90

Moreover, as the ground $^2E_2$' state is prone to the JT effect, the JT distortion path from D_{5h} to C_{2v} is followed by use of the Intrinsic Distortion Path (IDP) model, developed by one of us.[23-25] A short description can be found in the computational details section of SI. With this model, we were able to rationalize which normal modes contribute to the JT distortion, their contribution to the E_{JT} and how their contributions change along the IDP. The full results regarding the IDP treatment of $MnCp_2$ and $[FeCp_2]^+$ are presented in IDP section of SI, and only the main results and the

representation of the most important vibrations participating in the JT distortion, Figure 5, are presented here. Since the ground state has E_2' symmetry, the condition that $\langle\psi|\partial H/\partial q|\psi\rangle \neq 0$, imposes that normal modes (*q*) need to have e_1' symmetry (since in D_{5h}: $E_2' \otimes E_2' = A_1' + [A_2'] + E_1'$) and the first D_{5h} subgroup in which (one component of) these vibrations transform(s) as totally symmetric representation is C_{2v}. The analysis of the JT distortion in both $MnCp_2$ and $[FeCp_2]^+$ indicates that there are two identically highly significant vibrations that had to be taken into account when considering the JT distortions in these metal complexes. They are depicted in Figure 5, in the blue and red frame. The one at 150 cm^{-1} bends the two Cp rings and has the main influence on the JT distortion of both systems, but does not bring the dominant energetic contribution. This mode perfectly describes the sandwich opening in order to form a zigzag polymeric chain. Complementary to this, the vibration at approximately 450 cm^{-1} (ring tilt) additionally displaces the central metal ion and distorts the Cp planarity, and since it has a higher frequency, dominantly contributes to the E_{JT}. After further comparing the $MnCp_2$ and $[FeCp_2]^+$ it can be seen that manganocene has a larger E_{JT} and a somewhat larger distortion. More importantly, and present only in manganocene, there is one vibration of e_2' symmetry at 830cm^{-1} (Figure 5, green frame) that is important for the overall stabilization. This vibration has considerable force and energy contribution and approximately it corresponds to the difference in E_{JT} with regard to $[FeCp_2]^+$. Interestingly, this is not the JT active mode, and its true origin can be easily traced back to the pseudo-JT formalism (PJT).[37] The PJT effect takes into account the interactions with the excited states (of appropriate symmetry and energy separation relative to the ground state). Since our ground state is E_2', and, looking at the PJT contribution $\sum_i \langle\psi_0|\partial H/\partial q|\psi_i\rangle^2 / (E_0 - E_i)$, where the excited states are labeled by *i*, it is clear that acceptable ψ_i need to have E_1' or A_1' symmetry. It has been shown that the $^2E_2'/^2A_1'$ energy difference in $MnCp_2$ is -0.05 kcal·mol^{-1} while in $[FeCp_2]^+$ it is -5.5 kcal·mol^{-1}. Now, it becomes clear why this intriguing vibration is contributing only to the distortion in manganocene that have a low lying A'$_1$ state. The described e_2' mode mostly deforms angles inside Cp rings and, to a small extent, bond lengths. As Cp rings need to deform when they go from $MnCp_2$ to zigzag polymeric form (there are significant changes in angles and bond lengths because this process changes the hapticity), this vibration is the initial trigger that facilitates the conversion.

Finally, two different arrangements of five-membered anionic rings coordinated to metal ions, belonging to the D_{5h} and D_{5d} point groups will be discussed. In $MnCp_2$, the D_{5h} conformer is favored by ca. 1 kcal·mol^{-1}, while for $[FeCp_2]^+$ these two possibilities are almost isoenergetic and, thus, $MnCp_2$ is found in D_{5h}, but $[FeCp_2]^+$ is more often in the D_{5d} arrangement in crystal structures. When the IDP analysis was performed, it has been established that the distortion from the D_{5d} point is governed by only one (e_{1g}) dominant vibration (at 380 cm^{-1}), Figure 5, purple frame, but it does not lead to the desired bent crystal structure like in D_{5h} conformer, so the D_{5d} structure is not responsible for formation of the zigzag structure.

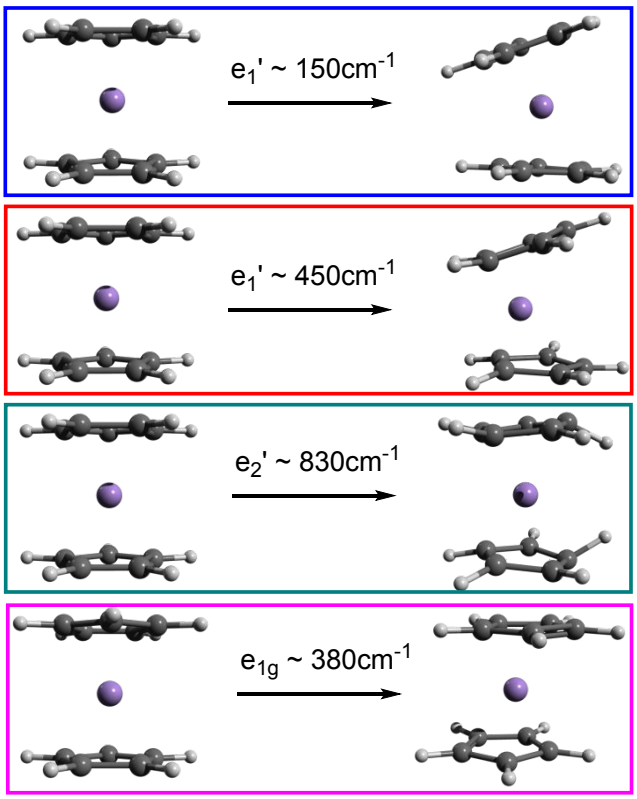

Figure 5. Four important JT active normal modes regarding the analysis of MCp_2 systems, in D_{5h} and D_{5d} symmetry.

The present work demonstrates that the peculiar behavior of manganocene is a consequence of three major factors: i) the JT active $^2E_2$' ground state that induces a distortion (Figure 5, blue frame, 150 cm^{-1}) that corresponds to the Cp bending which creates a zigzag polymer, ii) the close lying $^6A_1$' state that enables the conversion to the HS state present in the zigzag polymer, and, finally, iii) the close lying $^2A_1$' that facilitates the ligand deformation and triggers the polymerization. Only one of these three factors is present in any other metallocene complex, which sheds light on the peculiar behavior of manganocene that ironically does not follow the example of its homologue based on iron.

ASSOCIATED CONTENT

Supporting Information

The Supporting Information is available free of charge on the ACS Publications website.
The SI.pdf file contains additional Figures, the extended computational details, EDA analysis, IDP analysis.

AUTHOR INFORMATION

Corresponding Author

*E-mail: gmaja@chem.bg.ac.rs

Notes

The authors declare no competing financial interests.

ACKNOWLEDGMENT

We thank the Serbian Ministry of Education, Science and Technological Development (Grant No. 172035), MINECO (CTQ2017-87392-P), FEDER (UNGI10-4E-801), for financial support, and CSUC for extensive computer time.

REFERENCES

1. Ammeter, J. H.; Bucher, R.; Oswald, N., High-Spin-Low-Spin Equilibrium of Manganocene and Dimethylmanganocene. *J. Am. Chem. Soc.* **1974**, *96*, 7833-7835.
2. Layfield, R. A., Manganese(II): The Black Sheep of the Organometallic Family. *Chem. Soc. Rev.* **2008**, *37*, 1098-1107.
3. Swart, M., Metal–Ligand Bonding in Metallocenes: Differentiation between Spin State, Electrostatic and Covalent Bonding. *Inorganica Chim. Acta* **2007**, *360*, 179-189.
4. König, E.; Desai, V. P.; Kanellakopulos, B.; Klenze, R., Magnetic Properties of the Quasi One-Dimensional Heisenberg Linear Chain Antiferromagnet: Manganocene. *Chem. Phys.* **1980**, *54*, 109-113.
5. Walter, M. D.; Sofield, C. D.; Booth, C. H.; Andersen, R. A., Spin Equilibria in Monomeric Manganocenes: Solid-State Magnetic and EXAFS Studies. *Organometallics* **2009**, *28*, 2005-2019.
6. Cotton, F. A.; Wilkinson, G., *Advanced Inorganic Chemistry*. Wiley: 1999.
7. Walter, M. D.; Sofield, C. D.; Andersen, R. A., Spin Equilibria and Thermodynamic Constants for $(C_5H_4R)_2Mn$, R = H or Me, in Solid Solutions of Diamagnetic Diluents. *J. Organomet. Chem.* **2015**, *776*, 17-22.
8. Koehler, F. H.; Schlesinger, B., Spin Crossover, Dimerization, and Structural Dynamics of Manganocenes Probed by Deuterium NHR Spectroscopy. *Inorg. Chem.* **1992**, *31*, 2853-2859.
9. Reiners, M.; Baabe, D.; Schweyen, P.; Freytag, M.; Jones, P. G.; Walter, M. D., Teaching Ferrocenium How to Relax: A Systematic Study on Spin–Lattice Relaxation Processes in Tert-Butyl-Substituted Ferrocenium Derivatives. *Eur. J. Inorg. Chem.* **2017**, *2017*, 388-400.
10. Nawa, K.; Kitaoka, Y.; Nakamura, K.; Akiyama, T.; Ito, T., Electronic Configurations and Magnetic Anisotropy in Organometallic Metallocenes. *J. Appl. Phys.* **2015**, *117*, 17E131.
11. Nawa, K.; Kitaoka, Y.; Nakamura, K.; Imamura, H.; Akiyama, T.; Ito, T.; Weinert, M., Search for the Ground-State Electronic Configurations of Correlated Organometallic Metallocenes from Constraint Density Functional Theory. *Phys. Rev. B* **2016**, *94*, 035136.
12. Cirera, J.; Ruiz, E., Electronic and Steric Control of the Spin-Crossover Behavior in $[(CpR)_2Mn]$ Manganocenes. *Inorg. Chem.* **2018**, *57*, 702-709.
13. Salomon, O.; Reiher, M.; Hess, B. A., Assertion and Validation of the Performance of the B3LYP* Functional for the First Transition Metal Row and the G2 Test Set. *J. Chem. Phys.* **2002**, *117*, 4729-4737.
14. *Adf2013*, SCM, Theoretical Chemistry, Vrije Universiteit, Amsterdam, The Netherlands: Amsterdam, 2013.
15. Stepanovic, S.; Andjelkovic, L.; Zlatar, M.; Andjelkovic, K.; Gruden-Pavlovic, M.; Swart, M., Role of Spin-State and Ligand-Charge in Coordination Patterns in Complexes of 2,6-Diacetylpyridinebis(Semioxamazide) with 3d-Block Metal Ions: A Density Functional Theory Study. *Inorg. Chem.* **2013**, *52*, 13415-13423.
16. Swart, M.; Gruden, M., Spinning around in Transition-Metal Chemistry. *Acc. Chem. Res.* **2016**, *49*, 2690-2697.
17. Zlatar, M.; Gruden-Pavlović, M.; Güell, M.; Swart, M., Computational Study of the Spin-State Energies and UV-Vis Spectra of Bis(1,4,7-Triazacyclononane) Complexes of Some First-Row Transition Metal Cations. *Phys. Chem. Chem. Phys.* **2013**, *15*, 6631-6639.
18. Swart, M.; Ehlers, A. W.; Lammertsma, K., The Performance of OPBE. *Mol. Phys.* **2004**, *102*, 2467-2474.
19. Swart, M., Accurate Spin-State Energies for Iron Complexes. *J. Chem. Theory Comput.* **2008**, *4*, 2057–2066.
20. Gruden-Pavlović, M.; Stepanović, S.; Perić, M.; Güell, M.; Swart, M., A Density Functional Study of the Spin State Energetics of Polypyrazolylborato Complexes of First-Row Transition Metals. *Phys. Chem. Chem. Phys.* **2014**, *16*, 14514-14522.
21. Gruden, M.; Stepanovic, S.; Swart, M., Spin State Relaxation of Iron Complexes: The Case for OPBE and S12g Functionals. *J. Serb. Chem. Soc.* **2015**, *80*, 1399-1410.
22. Stepanovic, S.; Angelone, D.; Gruden, M.; Swart, M., The Role of Spin States in the Catalytic Mechanism of the Intra- and Extradiol Cleavage of Catechols by O_2. *Org. Biomol. Chem.* **2017**, *15*, 7860-7868.
23. Ramanantoanina, H.; Zlatar, M.; García-Fernández, P.; Daul, C.; Gruden-Pavlović, M., General Treatment of the Multimode Jahn–Teller Effect: Study of Fullerene Cations. *Phys. Chem. Chem. Phys.* **2013**, *15*, 1252-1259.
24. Zlatar, M.; Schläpfer, C.-W.; Penka Fowe, E.; Daul Claude, A., Density Functional Theory Study of the Jahn-Teller Effect in Cobaltocene. *Pure Appl. Chem.* **2009**, *81*, 1397–1411.
25. Zlatar, M.; Gruden-Pavlović, M.; Schläpfer, C.-W.; Daul, C., Intrinsic Distortion Path in the Analysis of the Jahn–Teller Effect. *THEOCHEM* **2010**, *954*, 86-93.
26. Swart, M.; Bickelhaupt, F. M., QUILD: Quantum-Regions Interconnected by Local Descriptions. *J. Comput. Chem.* **2008**, *29*, 724-734.
27. Haaland, A., The Molecular Structure of High-Spin Manganocene, $(n\text{-}C_5H_5)_2Mn$, by Gas Phase Electron Diffraction: A Rerefinement. *J. Inorg. Nucl. Chem. Lett.* **1979**, *15*, 267-269.
28. Reiher, M.; Salomon, O.; Hess, B. A., Reparameterization of Hybrid Functionals Based on Energy Differences of States of Different Multiplicity. *Theor. Chem. Acc.* **2001**, *107*, 48-55.
29. Paulsen, H.; Duelund, L.; Winkler, H.; Toftlund, H.; Trautwein, A. X., Free Energy of Spin-Crossover Complexes Calculated with Density Functional Methods. *Inorg. Chem.* **2001**, *40*, 2201-2203.
30. Xu, Z.-F.; Xie, Y.; Feng, W.-L.; Schaefer, H. F., Systematic Investigation of Electronic and Molecular Structures for the First Transition Metal Series Metallocenes $M(C_5H_5)_2$ (M = V, Cr, Mn, Fe, Co, and Ni). *J. Phys. Chem. A* **2003**, *107*, 2716-2729.
31. Swart, M., Spin States of (Bio)Inorganic Systems: Successes and Pitfalls. *Int. J. Quantum Chem.* **2013**, *113*, 2-7.
32. Harvey, J. Dft Computation of Relative Spin-State Energetics of Transition Metal Compounds. In *Principles and Applications of Density Functional Theory in Inorganic Chemistry I*; Springer Berlin Heidelberg: 2004; *Vol. 112*, Chapter 4, pp 151-184.
33. Phung, Q. M.; Vancoillie, S.; Pierloot, K., A Multiconfigurational Perturbation Theory and Density Functional Theory Study on the Heterolytic Dissociation Enthalpy of First-Row Metallocenes. *J. Chem. Theory Comput.* **2012**, *8*, 883-892.
34. Ammeter, J. H.; Oswald, N.; Bucher, R., Dynamische Jahn-Teller Verzerrungen Und Chemische Bindungsverhältnisse in Orbitalentarteten Sandwichkomplexen. *Helv. Chim. Acta* **1975**, *58*, 671-682.
35. Bucher R. Ph.D. Thesis: ESR-Untersuchungen an Jahn-Teller-Aktiven Sandwitchkomplexen. ETH Zürich, 1977.
36. Bickelhaupt, F. M.; Baerends, E. J. Kohn-Sham Density Functional Theory: Predicting and Understanding Chemistry. In *Reviews in Computational Chemistry*; Wiley-VCH, Inc.: 2000; *Vol. 15*.
37. Bersuker, I., *The Jahn-Teller Effect*. Cambridge University Press: Cambridge, 2006.

For Table of Contents Use Only

The Irony of Manganocene – An Interplay Between the Jahn-Teller Effect and Close Lying Electronic and Spin States

Stepan Stepanović, Matija Zlatar, Marcel Swart, Maja Gruden*

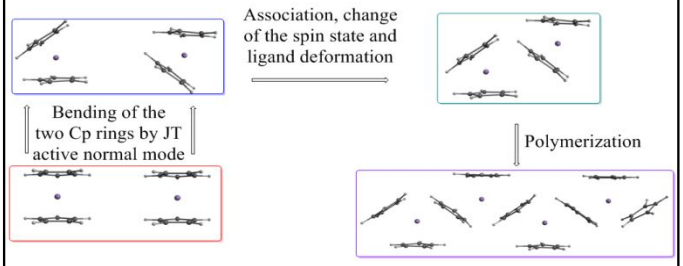

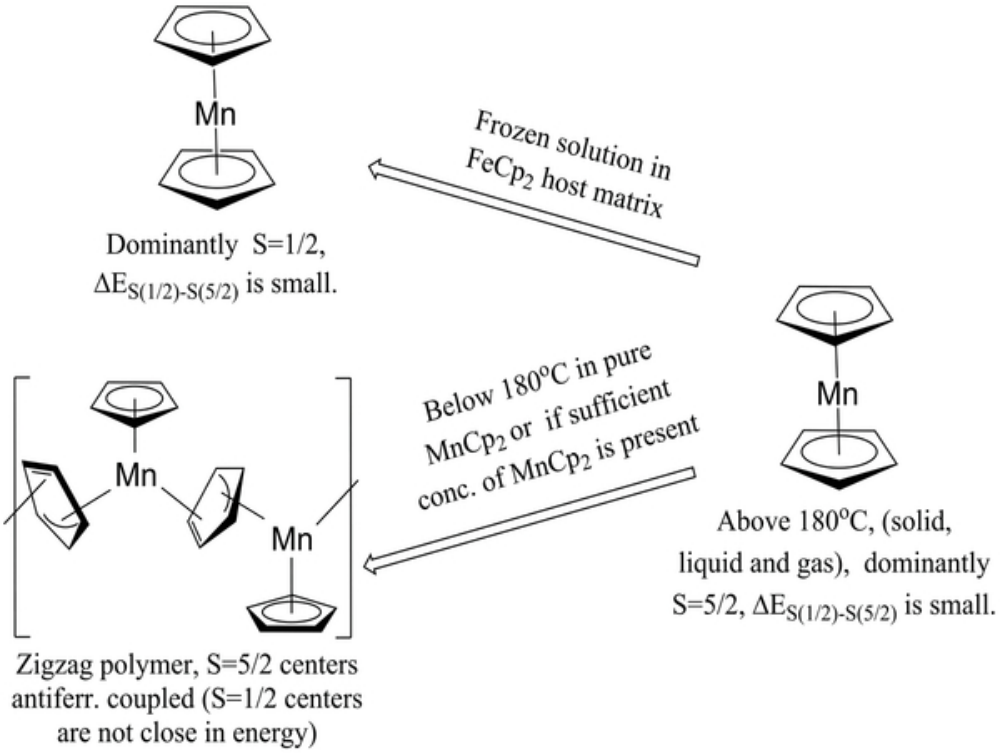

Figure 2. Schematic explanation of various forms of MnCp2

50x38mm (300 x 300 DPI)

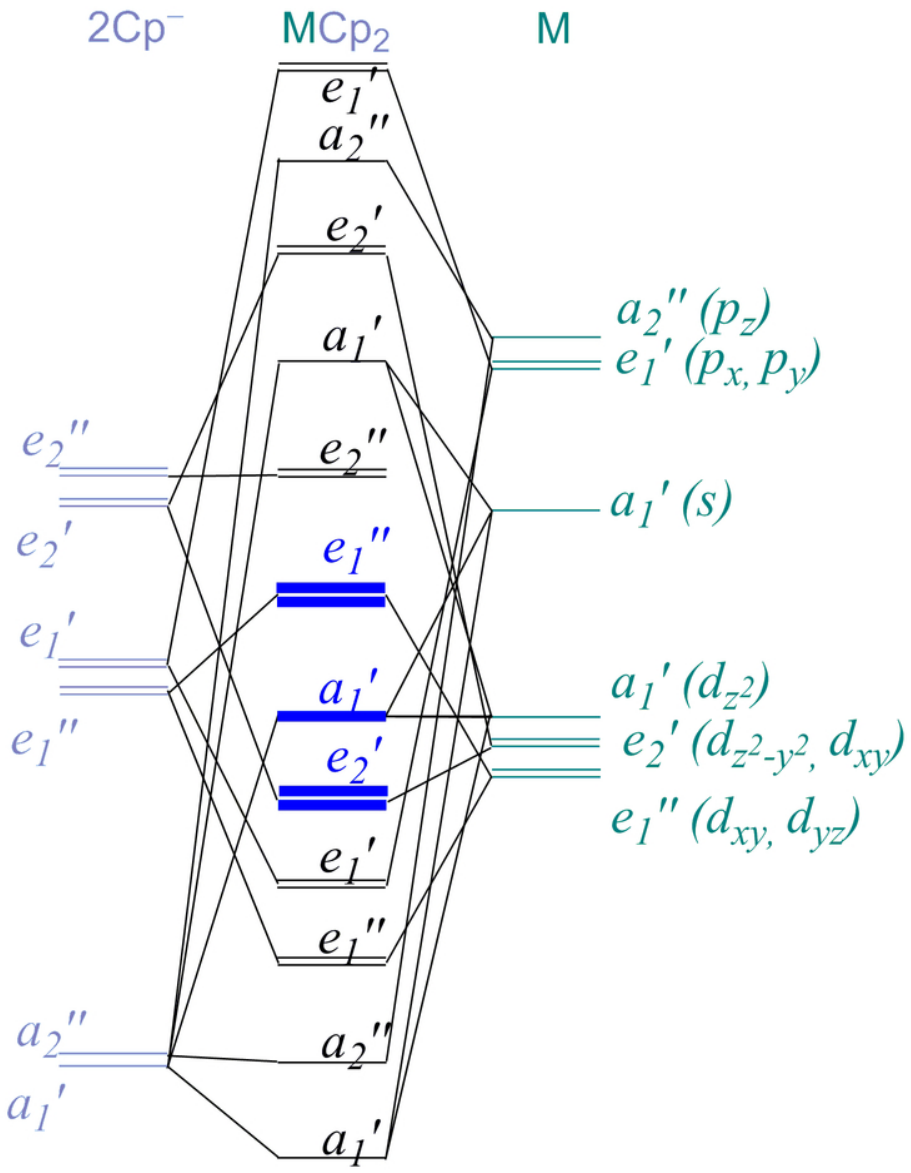

Figure 3. Qualitative MO diagram for metallocene sandwich compounds in D5h symmetry.

62x81mm (300 x 300 DPI)

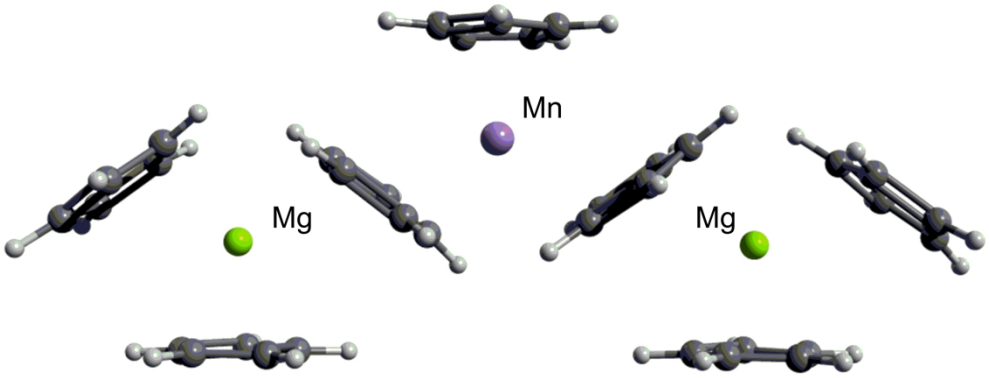

Figure 4. The model system used to estimate the HS/LS energy difference, on a single Mn2+ center in the zigzag structure.

237x95mm (300 x 300 DPI)

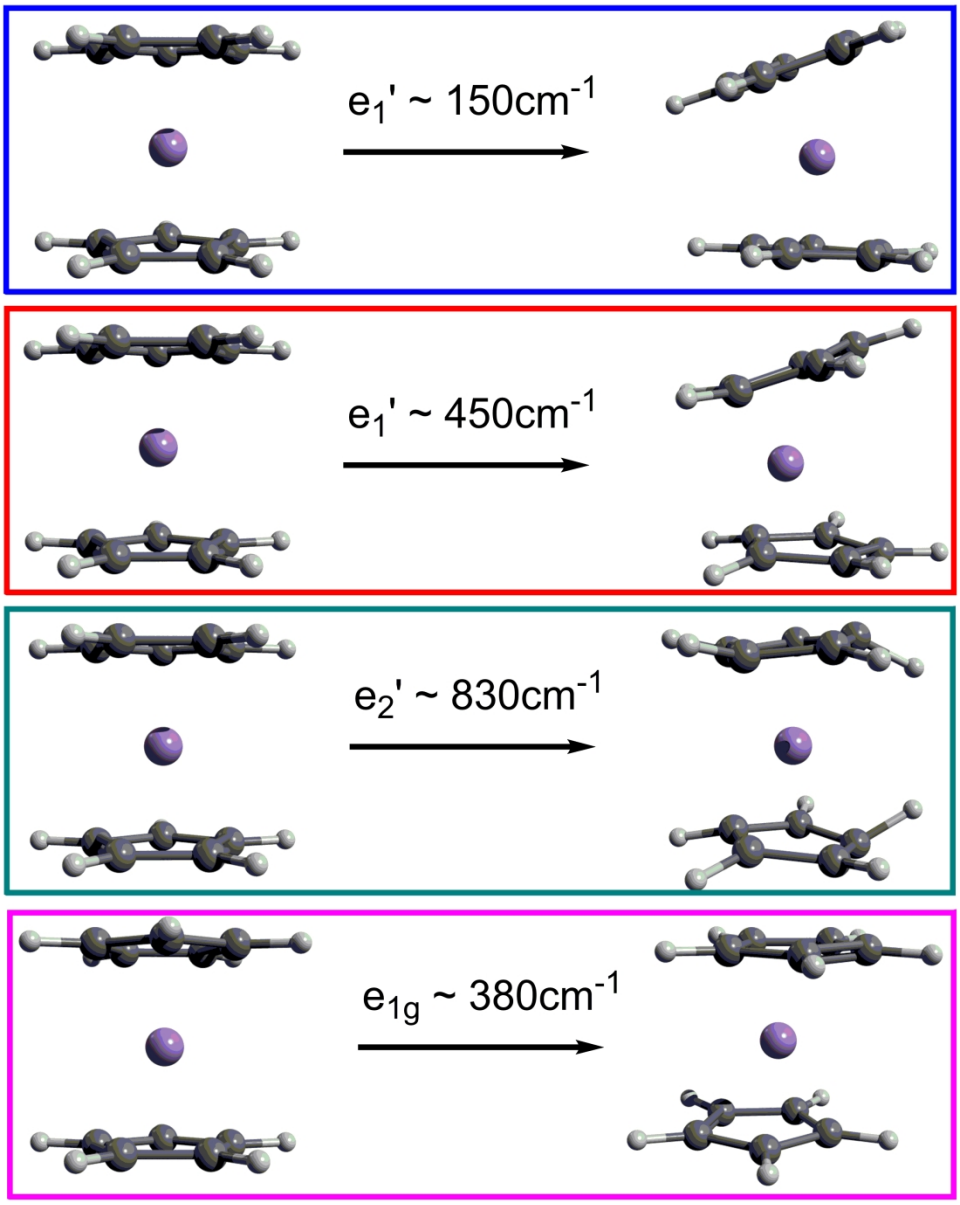

Figure 5. Four important JT active normal modes regarding the analysis of MCp2 systems, in D5h and D5d symmetry.

242x302mm (300 x 300 DPI)